

Rotation report

N-Acyl amides may be endogenous inducers of mitophagy

Author François Kroll

P.I. Hélène Plun-Favreau

Abstract

Mitophagy is the autophagic degradation of dysfunctional mitochondria. Loss-of-function mutations in key genes of the PINK1-dependent mitophagy pathway causes Mendelian forms of Parkinson's disease. At least three protective SNPs against Parkinson's have been shown to affect expression levels of PM20D1, an enzyme responsible for the synthesis and cleavage of *N*-Acyl amides, which are endogenous uncouplers of mitochondria. Incidentally, a decrease in mitochondrial potential is a clue to trigger mitophagy. We hypothesised this could be the mechanism behind the SNPs' protective effects: by mildly scaling down mitochondrial potential, these small metabolites could consistently induce slightly increased levels of mitophagy in individuals carrying the SNP(s). We first reproduced the uncoupling effects of one of these compounds in a human neuroblastoma cell line using TMRM staining. We then showed that a *N*-Acyl amide may be able to induce early mitophagy, as measured by phospho-ubiquitin levels and mitochondrial fragmentation. Being endogenous metabolites, *N*-Acyl amides could become promising clinical candidates as mild mitochondria uncouplers. We conclude by presenting the H4 astrocytoma cell line as a potentially more physiological model to study mitophagy in the brain.

Background

Mitophagy and Parkinson's disease

Mitophagy is the autophagic elimination of damaged mitochondria. Genome-wide association studies (GWAS) suggest a strong link between compromised mitophagy and Parkinson's disease (PD)¹.

PINK1 and parkin are among the most well-known proteins related to PD. Loss-of-function mutations in either of them lead to autosomal recessive forms of PD. PINK1 is a mitochondrial-targeted serine/threonine kinase, while parkin is an E3 ubiquitin ligase¹.

At least one pathway to mitophagy relies on PINK1-dependent activation of parkin. Healthy mitochondria maintain a high mitochondrial potential, which allows PINK1 to enter the inner mitochondrial membrane. There, PINK1 is cleaved by PARL. Conversely, damaged mitochondria typically lose their mitochondrial potential, which prevents PINK1 to be imported. It accumulates on the outer membrane, where it phosphorylates poly-ubiquitins. Phospho-ubiquitins (pUbs) trigger parkin recruitment to the mitochondria, where it also gets phosphorylated by PINK1.

Parkin's phosphorylation activates its ubiquitin E3 ligase activity. It ubiquitinates various proteins of the outer membrane such as mitofusins, which are subsequently phosphorylated by PINK1. This leads to a positive feedback loop where more pUbs lead to more parkin recruitment, which leads to more ubiquitins available to be phosphorylated by PINK1. Eventually, autophagy receptors like NDP52 and optineurin recognise phosphorylated ubiquitins and engage components of the autophagy pathway. An autophagosome is eventually formed around the damaged mitochondria and fuses with a lysosome, allowing the mitochondria to be degraded (**Figure 1**)²¹.

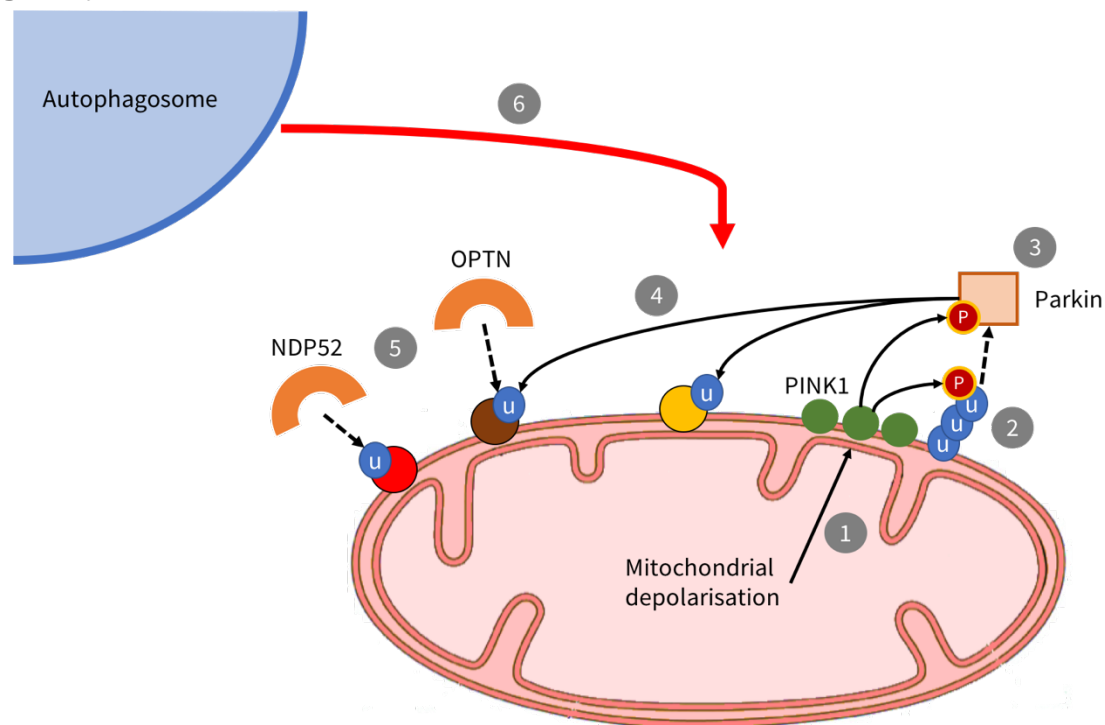


Figure 1 | PINK1-dependent mitophagy. Damaged mitochondria lose their mitochondrial potential (1). As a result, PINK1 accumulates on the outer membrane and phosphorylates poly-ubiquitins (2). Phospho-ubiquitins recruit parkin, which gets activated by PINK1 (3). Parkin ubiquitinates mitochondrial proteins (4), which recruit autophagy receptors (5). Finally, an autophagosome is formed and degrades the mitochondria (6). *Diagram courtesy of Asad Malik.*

PD SNPs lower PM20D1 expression

GWAS identified seven SNPs on 1q32 as significantly associated with PD. Interestingly, all seven are reportedly protective against PD, i.e. showing an odds ratio (OR) lower than 1 for the minor allele (OR = 0.71–0.75). Among them, rs947211 showed the strongest association with PD (p-value = 1.52×10^{-12})³.

Based on eQTL data^{4,5}, three of these seven SNPs correlate with a decreased expression of the protein PM20D1. For rs947211, this association is significant in the cerebellum and in most other tissues, such as liver and adipose tissue.

PM20D1 is a bidirectional enzyme: it both catalyses the condensation of an amino acid and a fatty acid, generating the corresponding *N*-Acyl amide (NAA), and their cleavage. NAAs are signalling metabolites which also are endogenous mitochondrial uncouplers. Their uncoupling mechanism likely involves binding to members of the SLC25 family, which have been shown to translocate protons across the inner membrane. Dissipation of the proton gradient produces heat, which is why PM20D1 is upregulated in beige adipose tissue after cold exposure in mice⁶.

Mitophagy and astrocytes

From three whole-brain RNA sequencing projects⁷⁻⁹, PM20D1 seems to be only expressed in modest levels in neurons while it seems significantly expressed in subsets of astrocytes, both in mouse and human. Furthermore, PM20D1 does not seem to be expressed at all in SH-SY5Y cells, the neuroblastoma line commonly used in mitophagy research¹⁰. Neuronal cell lines are thus probably not the appropriate model to study potential activities of PM20D1 in the brain.

More broadly, recent reports have questioned the attention given to neurons in PD pathogenesis and mitophagy. For instance, key PD-associated genes, including *pink1* and *parkin*, are expressed in astrocytes and have important roles in their function. PINK1 is important for astrocyte development, with *pink1*-knockout mouse brains exhibiting lower numbers of astrocytes. Parkin has also been shown to be important for astrocyte proliferation, unfolded protein response and inflammatory response. With regards to mitophagy specifically, knocking-out *parkin* in astrocytes has been shown to vastly increase the number of structurally damaged mitochondria, while no such increase was observed when knocking-out *parkin* in neurons¹¹. Finally, retinal ganglion neurons have been observed to transfer damaged mitochondria to neighbouring astrocytes for degradation, a process known as transmitophagy. This outsourcing of neuronal mitophagy to astrocytes is unlikely to be specific to the visual system as similar structures have been observed in the cerebral cortex¹².

Taken together, there is a need for an alternative non-neuronal cell model that can be used to study mitophagy. H4 is a human astrocytoma cell line which may be a good candidate as a convenient astrocyte-like cell model in which to monitor mitophagy^{13,14}.

Aims of the study

N-Acyl amides as potential endogenous inducers of mitophagy

We hypothesised that the protective mechanism behind the 1q32 PD-associated SNPs involve the modulation of the reaction catalysed by PM20D1. In summary, the SNPs would increase NAAs

concentrations by modulating the availability and/or affinity of PM20D1. Consequently, mitochondrial potential would constantly be slightly decreased in these individuals, inducing marginally higher levels of mitophagy.

Incidentally, the potential of mitochondrial uncouplers, mainly UCPs (uncoupling proteins), as neuroprotective has previously been explored in literature. For instance, leptin, a hormone produced by adipocytes, has been shown to protect neuroblastoma cells from toxicity generated by the complex I inhibitor MPP⁺ via upregulation of UCP2, which restored baseline mitochondrial potential after MPP⁺-induced hyperpolarisation¹⁵. Also of interest, *ucp-4* overexpression improved age-related neurodegeneration in *C. elegans*. However, neuroprotective effects were limited in *pink1*-knockout background, which supports our hypothesis that mild uncoupling induced by NAAs could be beneficial by stimulating PINK1-dependent mitophagy¹⁶.

We first set out to reproduce in a human neuroblastoma cell line the results by Long et al., 2016⁶ who showed an uncoupling effect of the NAA C18:1-Phe in hyperpolarised mitochondria. We also tested whether the compound at the same concentrations was able to uncouple basal mitochondrial potential. We then aimed to test if C18:1-Phe could induce mitophagy using immunostaining on pUb and TOM20.

H4 cells as an alternative model for mitophagy in the brain

In the goal of establishing H4 astrocytoma cells as a potentially more physiological model to study mitophagy in the human brain, we performed two experiments routinely performed to monitor mitophagy in the SH-SY5Y cells: immunostaining on pUb/TOM20 and siRNA knock-down followed by whole-cell lysate Western blot to detect PINK1 accumulation and mitochondrial proteins degradation.

Materials and methods

Cell culture

SH-SY5Y overexpressing FLAG-parkin were originally received from H. Ardley, Leeds Institute of Molecular Medicine¹⁷. They were cultured in Dulbecco's modified Eagle's medium (DMEM, 25 mM glucose) supplemented with 10% heat-inactivated foetal bovine serum (FBS) in a humidified chamber at 37 °C with 5% CO₂.

H4 astrocytoma cells were bought from ATCC® (#HTB-148™) and cultured exactly like SH-SY5Y cells.

Synthesis of the *N*-Acyl amide

Synthesis of the C18:1-Phe compound (*N*-oleoyl phenylalanine) was kindly performed by E. Bayle (Drug Discovery Institute, University College London) following Long et al.'s protocol⁶. The resulting white gritty solid was diluted in DMSO to generate a 10 mM stock, which was kept at 4°C prior to experiments.

Measurement of mitochondrial membrane potential

Mitochondrial membrane potential was measured using tetramethylrhodamine methyl ester fluorescence (TMRM, ThermoFisher Scientific, #T668). SH-SY5Y cells were grown onto glass coverslips in 6-well plates. They were then switched to HBSS (Hank's balanced salt solution: 156 mM NaCl, 3 mM KCl, 2 mM MgSO₄, 1.25 mM KH₂PO₄, 2mM CaCl₂, 10 mM glucose, 10 mM HEPES) containing 40 nM TMRM for 20 min before confocal imaging with a Zeiss 710 confocal microscope equipped with a 40× oil immersion objective. Compounds (1 μM oligomycin, 50 μM and 100 μM C18:1-Phe, 1 μM CCCP) were sequentially added directly onto the coverslip.

pUb/TOM20 immunostaining

This applies to both immunostaining on the SH-SY5Y and the H4 cells. Cells were grown on 96-well plates. Compounds were then added in the media at the indicated concentrations for the indicated lengths of time. Cells were fixed in 4% PFA, block and permeabilised (0.25% TritonX-100 in 10% FBS/PBS) before two-hour incubation with the primary antibodies (anti-pUb rabbit; anti-TOM20 mouse, 1:1000). Secondary antibodies (AlexaFluor 488 and 568, 1:2000) and Hoechst nuclear stain (1:2000) were incubated for one hour in the dark, before confocal imaging on the Opera Phenix (Perkin Elmer).

siRNA knock-down

H4 cells were reverse transfected following Dharmacon's protocol¹⁸ in 6-well plates with the corresponding siRNAs (ThermoFisher Scientific, 50 nM) using DharmaFECT 1 transfection reagent (Dharmacon, #T-2001, 0.48%).

SDS-PAGE and immunoblotting

H4 cells were incubated with a mix of 1 μM oligomycin A/1 μM antimycin A (Abcam, #ab143423; #ab141904) for 8 hours before whole-cell protein lysates were prepared using lysis buffer (50 mM Tris, 0.1 mM EGTA, 1 mM EDTA, 0.27 sucrose, 1% Triton-X, protease inhibitor, phosphatase inhibitor). After SDS-PAGE in NuPAGE™ 4-12% Bis-Tris protein gels, PVDF membranes were incubated overnight at 4°C with the primary antibodies (all 1:1000 except anti-TOM20): anti-PINK1 (#BC100-494), anti-mitofusin1 (#ab57602), anti-mitofusin2 (#ab56889), anti-GAPDH

(#9485), anti-PM20D1 (#ab186474), anti-TIMM23 (#ab116329), anti-TOM20 (#sc-17764, 1:2000). Secondary antibodies were the appropriate HRP-conjugated antibodies (#A0545; #A9044, 1:5000), incubated one hour at room temperature.

Kidney cells whole-cell lysates

Whole-cell lysates from immortalised human proximal tubule cells (HK-2), either treated or not with lipopolysaccharides (LPS) were kindly gave to us by Dr. David Sanders at the Institute of Nephrology, University College London.

Data analysis

All data analysis, statistics and plots were done in R¹⁹, with the occasional use of the R package ggplot2²⁰. In figures, one asterisk indicates a p-value ≤ 0.05 ; two asterisks a p-value ≤ 0.01 ; three asterisks a p-value ≤ 0.001 , as computed by Welch's t-test.

Results

N-Acyl amides modulate mitochondrial potential in human neuroblastoma cells

Long et al., 2016⁶ reported an uncoupling effect of the NAA C18:1-Phe in a mouse myoblast cell line after hyperpolarisation of the mitochondria by oligomycin. We first aimed to reproduce these results in SH-SY5Y cells, a human neuroblastoma cell line, together with testing if this NAA could uncouple basal mitochondrial potential at the same concentrations.

We performed TMRM staining on SH-SY5Y cells overexpressing FLAG-Parkin. TMRM is a dye which accumulates to the mitochondria in proportion to their membrane potential: the higher the mitochondrial potential, the brighter the TMRM signal²¹. While Long et al. used FACS to quantify TMRM staining, we used confocal microscopy. This gave us the opportunity to monitor TMRM staining continuously across time and successive treatments, and not at one specific timepoint.

As expected, treatment with oligomycin (1 μM) increased mitochondrial potential. Oligomycin blocks the proton channel of the ATP synthase. Protons imported from the matrix by the electron transport chain thus accumulate in the intermembrane space, raising mitochondrial potential. Surprisingly, addition of 50 μM of C18:1-Phe seemed to further hyperpolarised mitochondria: TMRM signal increased more than twice as fast after adding the NAA than after adding oligomycin (slope = 0.07 after oligomycin vs 0.17 after 50 μM C18:1-Phe). Addition of 100 μM of C18:1-Phe eventually depolarised membrane potential after a short plateau (slope = -0.15 between 25 and 31 min). After 10 minutes of incubation with 100 μM of C18:1-Phe, mitochondrial potential was back to levels around those obtained after addition of oligomycin alone, essentially reproducing Long et al.'s results. Before the end of the timecourse, 1 μM of CCCP was added to show definite depolarisation of the mitochondria. CCCP is a potent ionophore which essentially acts as an extreme uncoupler instantly dissipating the proton gradient (slope = -1.04 just after adding CCCP) (**Figure 2**).

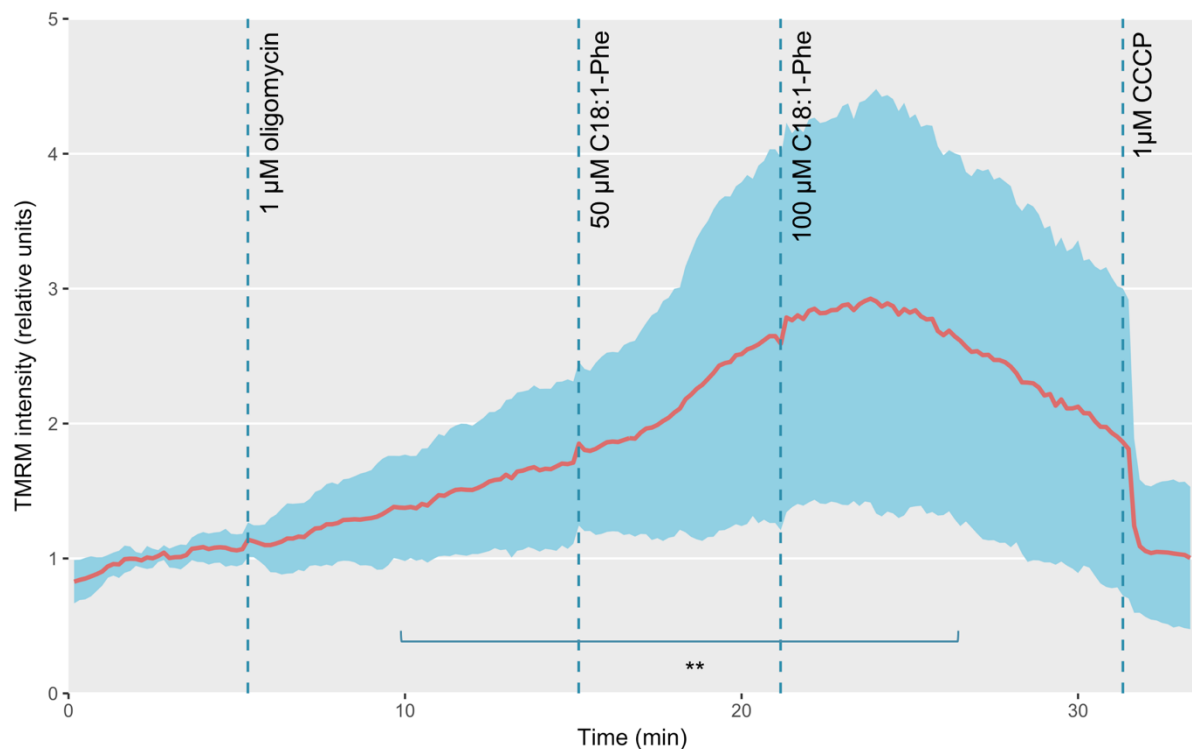


Figure 2 | Mitochondrial potential timecourse measured by TMRM staining, represented as mean across 15 cells (orange line) \pm standard deviation (blue error band). Signal intensity was normalised to baseline (mean of the first 5.3 min). 100 μM C18:1-Phe significantly depolarised mitochondria after hyperpolarisation induced by 1 μM oligomycin (p -value = 0.006).

In a second version of this experiment, we first added C18:1-Phe at the same concentrations to test if the NAA was able to uncouple basal mitochondrial potential.

Initial addition of 50 μM of C18:1-Phe did not seem to have any significant effect on mitochondrial potential (slope during baseline = -0.01 vs slope after 50 μM C18:1-Phe = 0.00). Next, addition of 100 μM of C18:1-Phe significantly hyperpolarised mitochondria (slope after 100 μM C18:1-Phe = 0.04). Addition of oligomycin did not seem to further increase hyperpolarisation: TMRM signal intensity continued to slowly increase (slope after oligomycin = 0.06), which confirms that the NAA counteracts the effect of oligomycin. Finally, addition of 1 μM CCCP acutely uncoupled mitochondria as expected (slope just after adding CCCP = -1.7) (**Figure 3**).

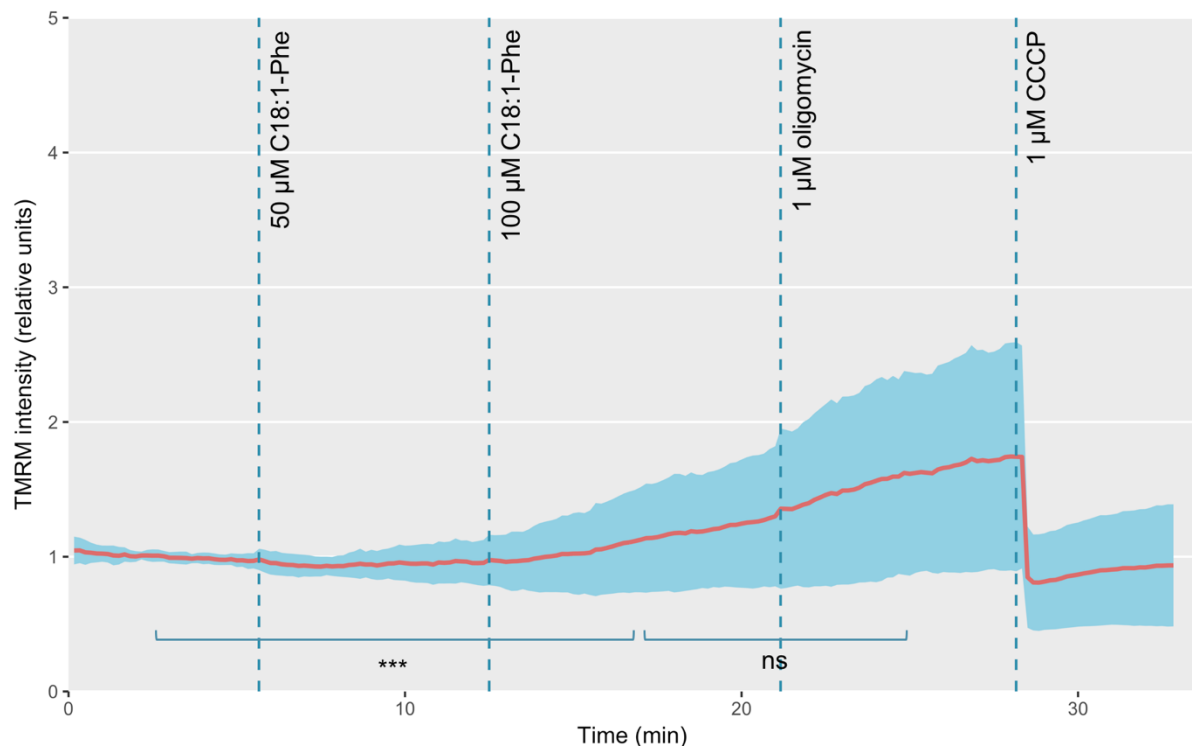


Figure 3 | Mitochondrial potential timecourse measured by TMRM staining (see legend of **Figure 2** for details). 100 μM C18:1-Phe significantly hyperpolarised the mitochondria compared to baseline (p-value = 0.0002), and 1 μM oligomycin did not affect this increase (p-value = 0.45).

N-Acyl amides may trigger mitophagy

We then set out to test if C18:1-Phe could induce mitophagy in the SH-SY5Y cells overexpressing FLAG-Parkin. This was done by immunostaining on pUb and TOM20. We measure the former as a proxy for early activation of mitophagy, while the latter is used to monitor downstream degradation of mitochondria. Intense induction of mitophagy, as achieved for instance by 3 hours of exposition to a mix of oligomycin/antimycin, will strongly increase signal in the pUb channel and decrease signal in the TOM20 channel (**Supplementary figure 1**). While oligomycin blocks ATP synthase, antimycin inhibits complex III of the electron transport chain. The combined effect is dissipation of the mitochondrial proton gradient, which triggers mitophagy.

100 μ M of C18:1-Phe seemed to significantly raise pUb levels, both after 3 hours (data not shown) and 6 hours exposition (**Figure 5**). We were unable to detect a TOM20 decrease in this timeframe (data not shown). These results need to be taken with a lot of caution. Indeed, cell number was significantly diminished in the wells treated with 100 μ M C18:1-Phe (**Supplementary figure 2**), which may bias comparisons. More importantly, it would also indicate that 100 μ M is excessive and may induce cell death, potentially due to excessive uncoupling.

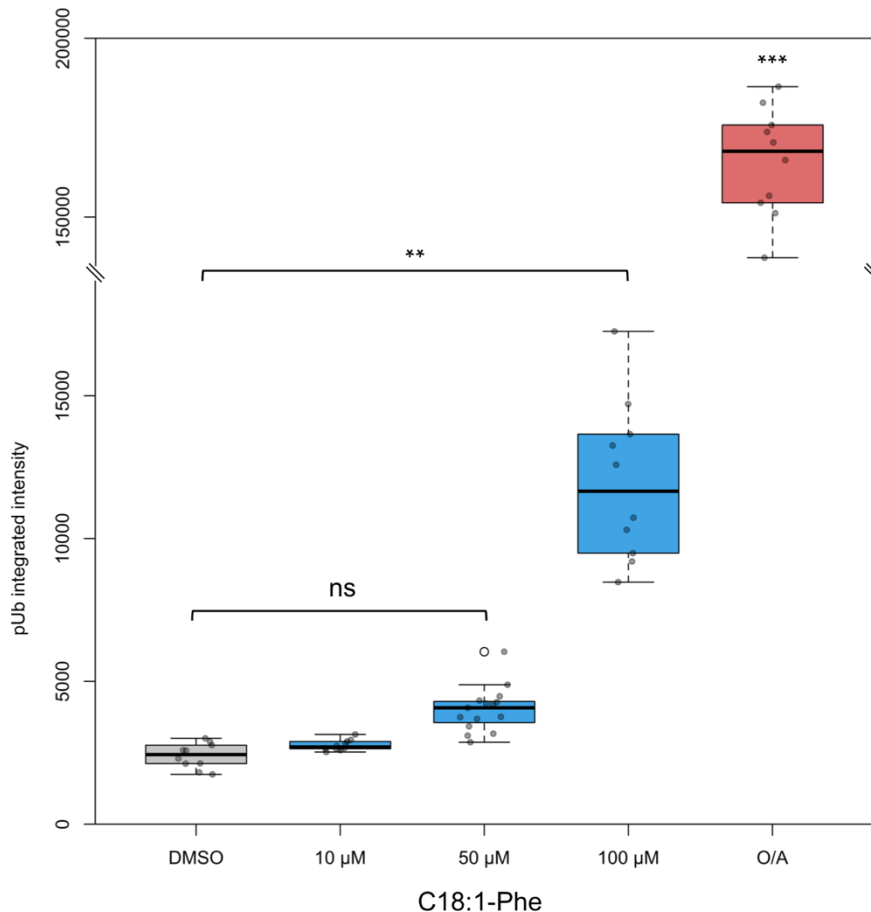


Figure 4 | pUb signal intensity in SH-SY5Y cells incubated with C18:1-Phe for 6 hours. 100 μ M C18:1-Phe significantly increased pUb integrated intensity (p-value = 0.0013). 1 μ M oligomycin/antimycin is used here as a control to show strong induction of mitophagy (p-value \sim 0). N = 10 wells/treatment.

Astrocytoma cells as an alternative model to study mitophagy

Mitophagy in H4 cells can be manipulated by siRNA and detected by Western blot

A method commonly used to study mitophagy in the SH-SY5Y cells is to knock-down specific genes of the pathway using siRNAs before inducing mitophagy by exposition to oligomycin/antimycin and probing for mitochondrial proteins in whole-cell lysate Western blot.

We assessed here if this was also possible in the H4 astrocytoma cells. In addition, we tested if we could detect PM20D1 in these cells.

Mitophagy could be detected in H4 cells after 8 hours oligomycin/antimycin exposition. This is clear when looking at PINK1 accumulation and decreased mitofusins 1 and 2. We were also able to knock-down PINK1 using siRNA, preventing its accumulation (**Figure 5**).

Interestingly, mitofusins 1 and 2 are distinctly being degraded even when PINK1 is knocked-down. This raises the question that PINK1-independent mitophagy pathways could be activated in these cells to compensate for the shortage of PINK1. It is however unclear if TOM20 and/or TIM23 degradation could be observed here.

Finally, whether we were able to detect PM20D1 in the H4 cells remains ambiguous. Assuming that the PM20D1 siRNA worked, the band we observed is unlikely to be PM20D1 as it does not show any decrease in the knock-down. This band also seems to be present in the SH-SY5Y cells, which is not expected based on RNAseq data. As PM20D1 is highly expressed in mouse and human kidney, we added here lysates from human kidney cells (HK-2) to serve as a positive control for the antibody. The slightly lower, more compact band in these cells may be PM20D1, although the band is predicted lower, around 56 kDa²². Overall, more tests should be performed to confirm the antibody's specificity (**Figure 5**).

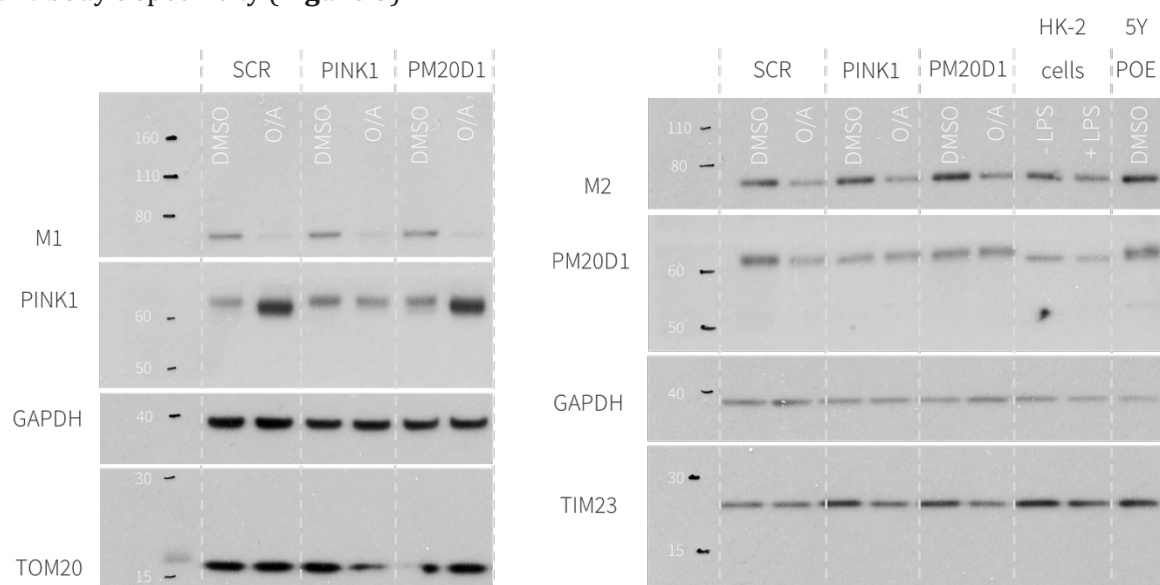


Figure 5 | Detection of mitophagy in the H4 cells by immunoblotting. On the left are the primary antibodies used; on top are either which siRNAs were used to knock-down the specified gene (eg. PINK1 is PINK1-knockdown) or which cells the lysate was from (only for HK-2 and 5Y POE cells). SCR, scrambled siRNA, M1, mitofusin 1; M2, mitofusin 2; O/A, oligomycin/antimycin; 5Y POE, SH-SY5Y FLAG-Parkin overexpressing. Mass markers are in kDa. GAPDH is probed here as loading control. Representative of two independent experiments.

Early mitophagy can be detected by immunostaining in H4 cells

Another method routinely used to detect mitophagy in the SH-SY5Y cells is confocal imaging of fixed cells where pUb and TOM20 are fluorescently stained by immunostaining.

To test whether this could also be performed in the H4 astrocytoma cells, we performed a timecourse of oligomycin/antimycin exposition.

We were able to detect a clear induction of pUb proportional to the time of oligomycin/antimycin exposition. Although we did not observe a decrease in the TOM20 signal within this timeframe, we could detect what seems to be mitochondrial fragmentation, as measured by the number of spots of TOM20 staining (**Supplementary figure 3**). Fragmentation indeed precedes engulfment by autophagosomes, as these are up to five times smaller than mitochondria²³. Based on this chronology, it is likely that a TOM20 decrease can be detected within a longer timeframe.

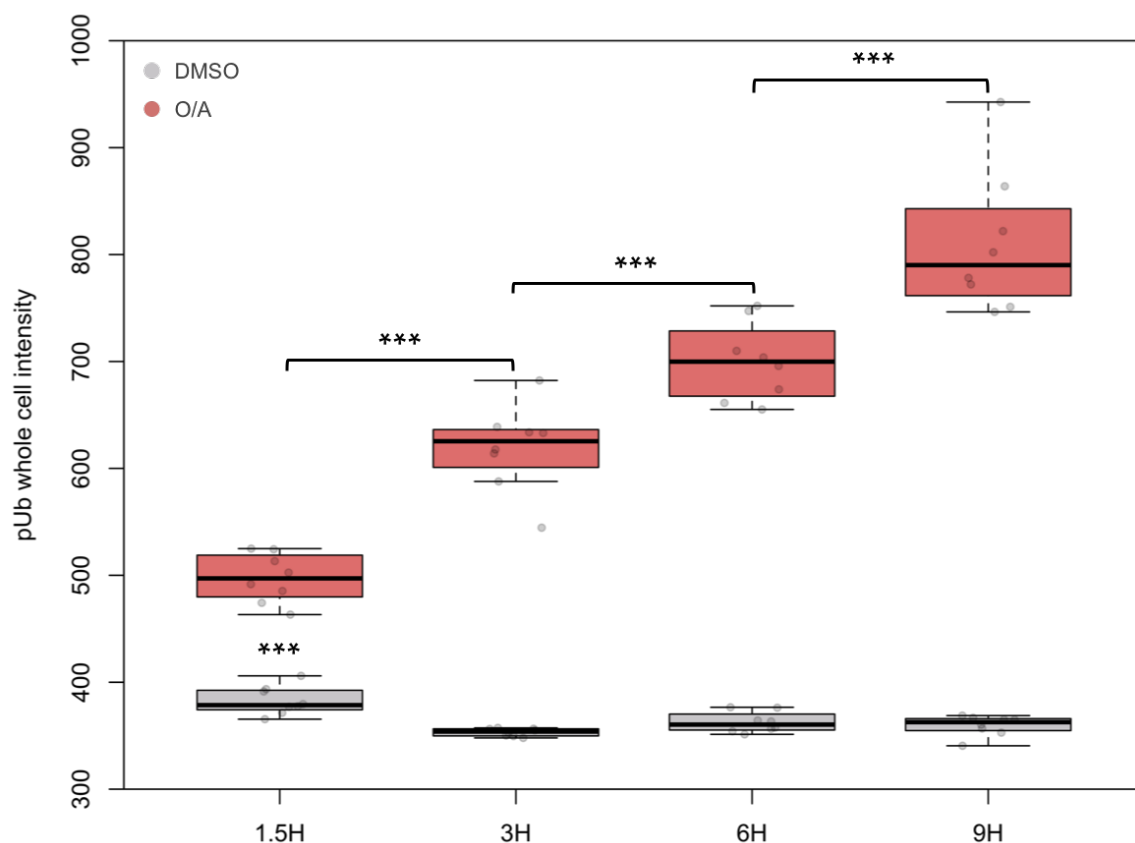


Figure 6 | Timecourse of pUb signal intensity as a function of treatment time in the H4 astrocytoma cells. Differences between treated and non-treated (DMSO) and increases between timepoints within the O/A-treated wells were all highly significant (p-values < 0.0001). N = 8 wells/timepoint and treatment.

Discussion

First of all, we were broadly able to reproduce the uncoupling effect of the NAA C18:1-Phe in the human neuroblastoma cells. Surprisingly, the uncoupling is preceded by a hyperpolarisation in these cells. Either this is a cell-specific effect of the compound or Long et al. missed it by looking at one specific timepoint. As a consequence, the uncoupling mechanism in the SH-SY5Y cells is unlikely to be as straightforward as direct activation of the SLC25 channels. Additionally, we did not observe depolarisation of basal mitochondrial potential upon addition of C18:1-Phe. However, this compound was later shown to uncouple respiration at 50 μM ²⁴. The basal uncoupling effect is thus likely to be true. Assuming this is not explained by differences in cell lines, it is possible that the timeframes we used here were not long enough.

Although these results need to be thoroughly checked due to the potential bias of cell number, C18:1-Phe did seem to induce an increase in pUb staining, which we use as a proxy for early trigger of mitophagy. This may support the mild uncoupling hypothesis of the 1q32 protective SNPs. However, information concerning PM20D1 are insufficient to confidently place this in a broader mechanism for the SNPs. Plasma concentrations of NAAs are very low (3.8 ± 0.4 nM for C18:1-Phe)⁶, which makes it almost impossible that NAAs produced by PM20D1 in distant tissues such as kidney or adipose tissue affect mitophagy in the brain. The pathway is thus likely to occur locally. In our context, NAAs could directly be produced by the populations of astrocytes expressing PM20D1, affecting mitophagy in the neighbouring cells.

Finally, our two proof-of-concepts experiments demonstrated that mitophagy could be induced and detected in the H4 astrocytoma cells. Interestingly, knocking-down PINK1 did not seem to affect degradation of mitofusins in our immunoblotting experiments, which suggest alternative pathways. PINK1-independent mitophagy was demonstrated in an asymptomatic carrier of a parkin mutation²⁵, flies²⁶, and mice²⁷, which also highlights the potential bias introduced when using SH-SY5Y cells overexpressing FLAG-parkin: by flooding the cell with parkin, cells may be over-relying on PINK1-dependent mitophagy in a non-physiological manner.

Future directions

An original direction for this work would be to move to a non-mammalian animal model, for instance zebrafish (*Danio rerio*). The so-called MitoFish is a reporter line where specific populations of neuronal mitochondria are fluorescently tagged²⁸. Using this line, it may be possible to monitor mitochondrial degradation using time-lapse confocal microscopy in an intact organism. NAA compounds can probably be administered by simple addition in the water, and

PINK1 can be knocked-down using a Morpholino to test whether potential benefits are PINK1-dependent²⁹. Mitochondrial respiration assays can even be performed in a high-throughput manner on intact embryos in 96-well plates to test the uncoupling abilities of the combinatorial number of NAAs³⁰.

In a broader perspective, assuming that mild mitochondrial uncoupling is indeed beneficial against PD, NAAs could represent strong clinical candidates: being endogenous metabolites, they are likely to be well-tolerated.

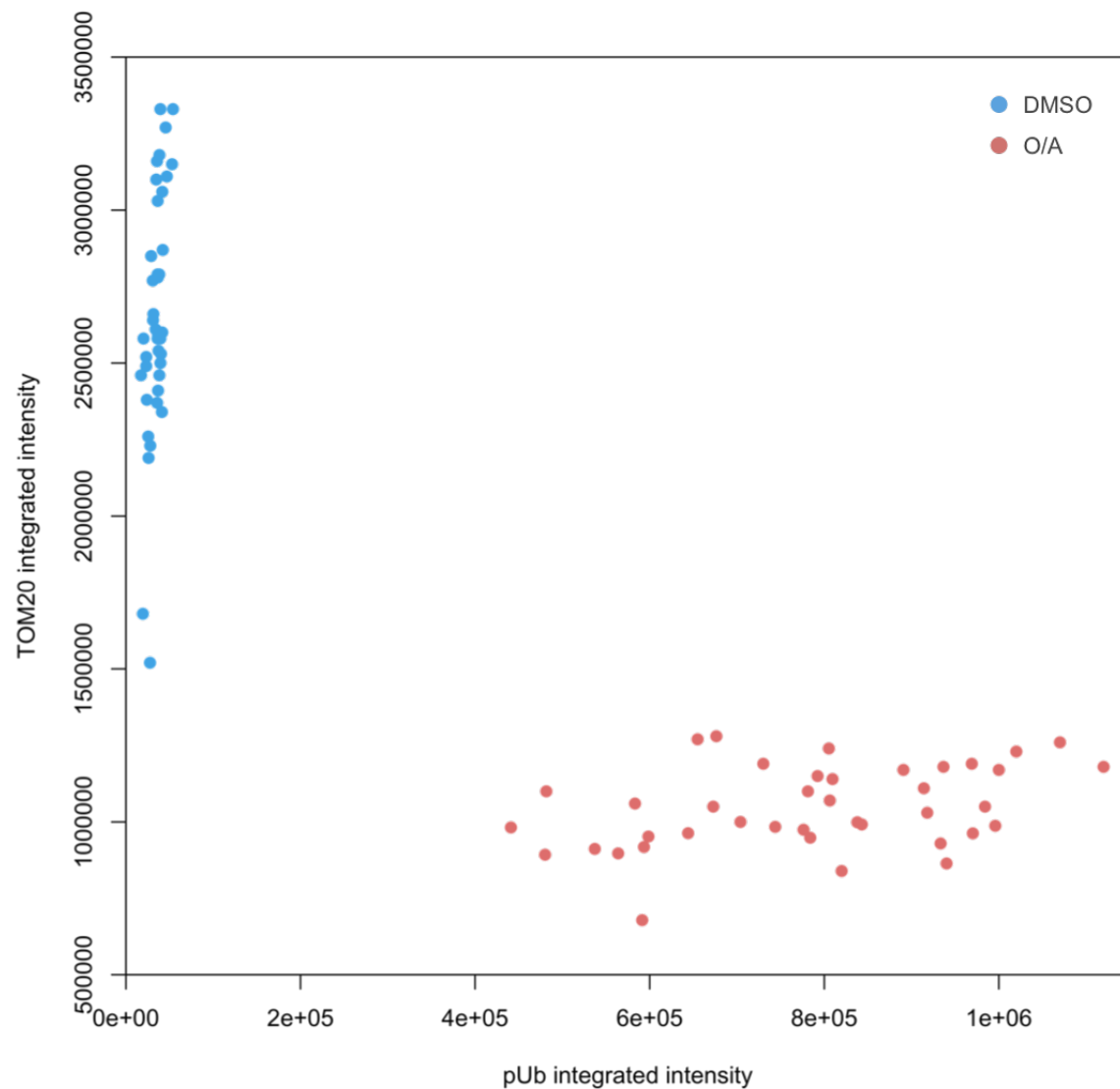
References

1. Gao, F. *et al.* Mitophagy in Parkinson's Disease: Pathogenic and Therapeutic Implications. *Front. Neurol.* **8**, 527 (2017).
2. Matsuda, N. Phospho-ubiquitin: upending the PINK–Parkin–ubiquitin cascade. *J. Biochem.* **159**, 379–385 (2016).
3. Satake, W. *et al.* Genome-wide association study identifies common variants at four loci as genetic risk factors for Parkinson's disease. *Nat. Genet.* **41**, 1303–1307 (2009).
4. UK Brain Expression Consortium (UKBEC). Braineac. (2018). Available at: <http://www.braineac.org/>. (Accessed: 8th May 2018)
5. Broad Institute. GTExPortal. (2018).
6. Long, J. Z. *et al.* The Secreted Enzyme PM20D1 Regulates Lipidated Amino Acid Uncouplers of Mitochondria. *Cell* **166**, 424–435 (2016).
7. Zeisel, A. *et al.* Molecular architecture of the mouse nervous system. *bioRxiv* 294918 (2018). doi:10.1101/294918
8. Saunders, A. *et al.* A Single-Cell Atlas of Cell Types, States, and Other Transcriptional Patterns from Nine Regions of the Adult Mouse Brain. *bioRxiv* 299081 (2018). doi:10.1101/299081
9. Zhang, Y. *et al.* An RNA-sequencing transcriptome and splicing database of glia, neurons, and vascular cells of the cerebral cortex. *J. Neurosci.* **34**, 11929–47 (2014).
10. Harenza, J. L. *et al.* Transcriptomic profiling of 39 commonly-used neuroblastoma cell lines. *Sci. Data* **4**, 170033 (2017).
11. Booth, H. D. E., Hirst, W. D. & Wade-Martins, R. The Role of Astrocyte Dysfunction in Parkinson's Disease Pathogenesis. *Trends Neurosci.* **40**, 358–370 (2017).
12. Davis, C. O. *et al.* Transcellular degradation of axonal mitochondria. *Proc. Natl. Acad. Sci. U. S. A.* **111**, 9633–8 (2014).
13. ExPASy. Cellosaurus H4 (CVCL_1239). (2018). Available at: https://web.expasy.org/cellosaurus/CVCL_1239. (Accessed: 9th May 2018)
14. ATCC®. H4 (ATCC® HTB-148™). (2016). Available at: <https://www.lgcstandards-atcc.org/Products/All/HTB-148.aspx>. (Accessed: 9th May 2018)
15. Ho, P. W.-L. *et al.* Mitochondrial Uncoupling Protein-2 (UCP2) Mediates Leptin Protection Against MPP+ Toxicity in Neuronal Cells. *Neurotox. Res.* **17**, 332–343 (2010).
16. Cho, I., Song, H.-O. & Cho, J. H. Mitochondrial Uncoupling Attenuates Age-Dependent Neurodegeneration in *C. elegans*. *Mol. Cells* **40**, 864–870 (2017).
17. Ardley, H. C. *et al.* Inhibition of proteasomal activity causes inclusion formation in neuronal and non-neuronal cells overexpressing Parkin. *Mol. Biol. Cell* **14**, 4541–56 (2003).
18. GE Healthcare. Dharmacon™ Reverse Transfection of siRNA. (2018). Available at: <http://dharmacon.horizondiscovery.com/uploadedFiles/Resources/reverse-transfection-sirna-of-sirna-protocol.pdf>. (Accessed: 9th May 2018)
19. R Core Team. R: A Language and Environment for Statistical Computing. (2017).
20. Wickham, H. *ggplot2: Elegant Graphics for Data Analysis*. (2009).
21. ThermoFisher Scientific. Tetramethylrhodamine (TMRM). Available at: <https://www.thermofisher.com/order/catalog/product/T668>.
22. Abcam. Anti-PM20D1 antibody - N-terminal (ab186474). (2018). Available at:

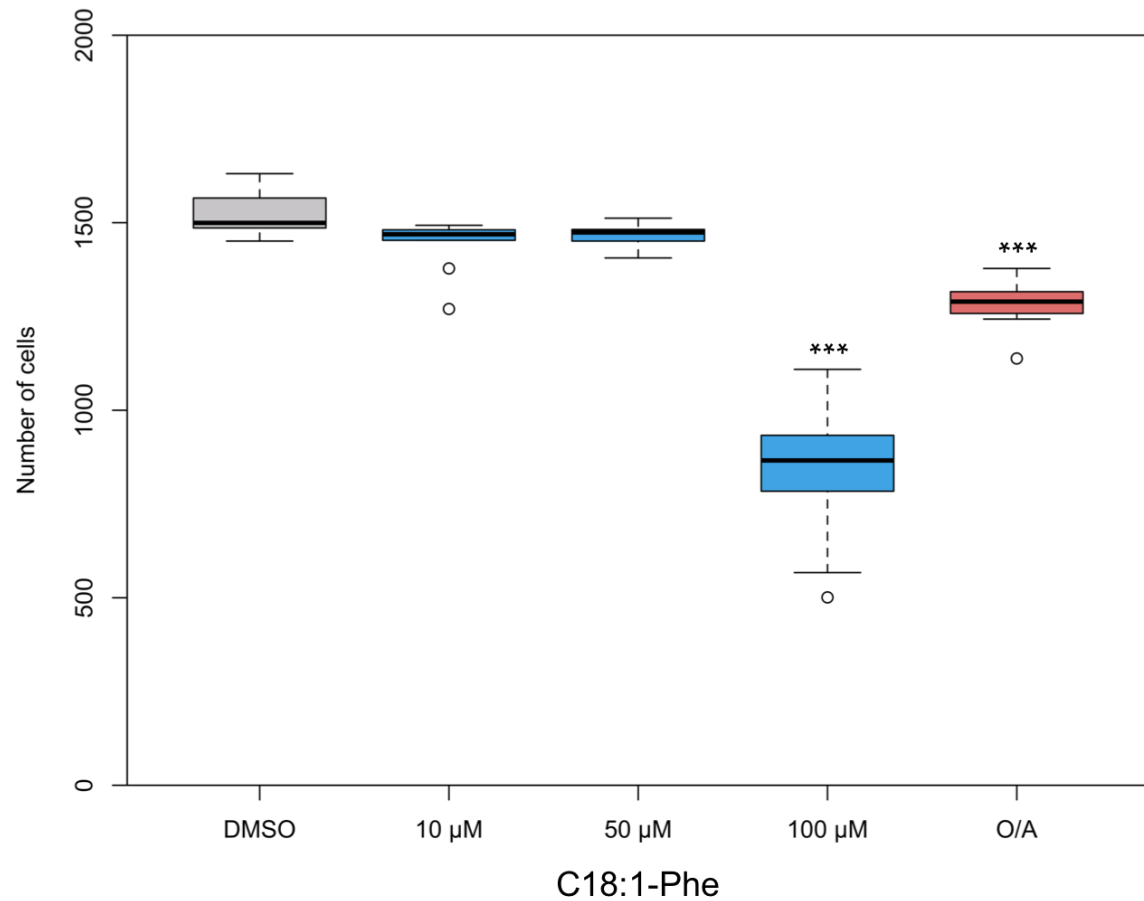
http://www.abcam.com/pm20d1-antibody-n-terminal-ab186474.html#description_images_1.
(Accessed: 9th May 2018)

23. Gomes, L. C. & Scorrano, L. Mitochondrial morphology in mitophagy and macroautophagy. *Biochim. Biophys. Acta - Mol. Cell Res.* **1833**, 205–212 (2013).
24. Keipert, S. *et al.* Long-Term Cold Adaptation Does Not Require FGF21 or UCP1. *Cell Metab.* **26**, 437–446.e5 (2017).
25. Koentjoro, B., Park, J.-S. & Sue, C. M. Nix restores mitophagy and mitochondrial function to protect against PINK1/Parkin-related Parkinson's disease. *Sci. Rep.* **7**, 44373 (2017).
26. Lee, J. J. *et al.* Basal mitophagy is widespread in *Drosophila* but minimally affected by loss of Pink1 or parkin. *J. Cell Biol.* **217**, 1613–1622 (2018).
27. McWilliams, T. G. *et al.* Basal Mitophagy Occurs Independently of PINK1 in Mouse Tissues of High Metabolic Demand. *Cell Metab.* **27**, 439–449.e5 (2018).
28. Plucińska, G. *et al.* In vivo imaging of disease-related mitochondrial dynamics in a vertebrate model system. *J. Neurosci.* **32**, 16203–12 (2012).
29. Anichtchik, O. *et al.* Loss of PINK1 function affects development and results in neurodegeneration in zebrafish. *J. Neurosci.* **28**, 8199–207 (2008).
30. Shim, J. *et al.* Triclosan is a mitochondrial uncoupler in live zebrafish. *J. Appl. Toxicol.* **36**, 1662–1667 (2016).

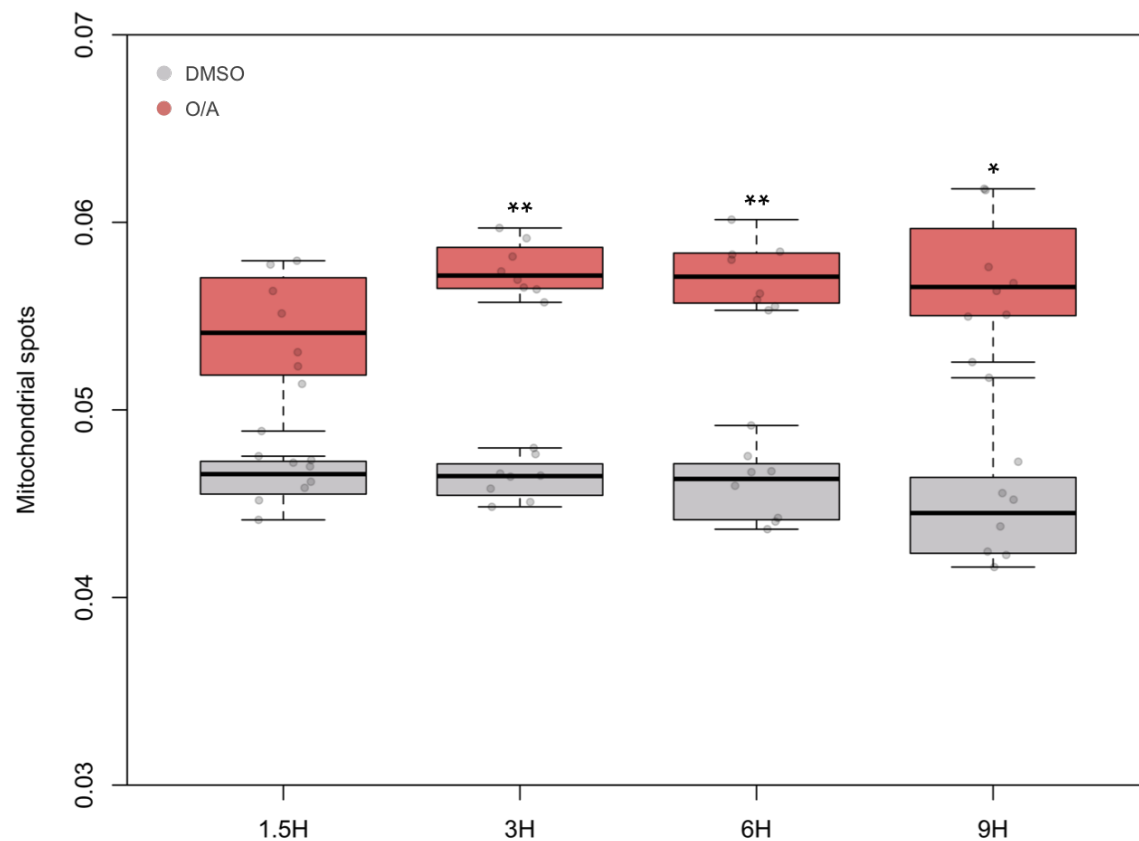
Supplementary data



Supplementary figure 1 | Induction of mitophagy by exposition to oligomycin/antimycin in SH-SY5Y cells overexpressing FLAG-parkin. After a 3-hour treatment with oligomycin/antimycin (orange dots), signal intensity in the pUb channel is strongly increased, while signal in the TOM20 channel is greatly diminished compared to control wells treated with DMSO (blue dots).



Supplementary figure 2 | Number of SH-SY5Y cells in the field of view after 6-hour treatment with the indicated compound. Wells treated with 100 μM C18:1-Phe and oligomycin/antimycin (O/A) contained significantly less cells compared to wells treated with DMSO (p-values < 0.001).



Supplementary figure 3 | Increase in mitochondrial spots after oligomycin/antimycin treatment in the H4 cells. All differences between DMSO and oligomycin/antimycin treated were highly significant (p-values $< 10^{-7}$). Differences between 1.5 hours treatment and longer timepoints were also significant (p-values < 0.02).